TECHNICAL MEMORANDUM

X - 61

WIND-TUNNEL INVESTIGATION OF PRESSURES AND HINGE MOMENTS ON A SWEPTBACK T-MOUNTED HORIZONTAL TAIL AT MACH NUMBERS FROM 0.60 TO 1.075

By Robert J. Ward and Joseph M. Hallissy, Jr.

Langley Research Center
Langley Field, Va.

Declassified October 16, 1961

NATIONAL AERONAUTICS AND SPACE ADMINISTRATION
WASHINGTON

November 1959

NATIONAL AERONAUTICS AND SPACE ADMINISTRATION

TECHNICAL MEMORANDUM X-61

WIND-TUNNEL INVESTIGATION OF PRESSURES AND HINGE MOMENTS ON A SWEPTBACK T-MOUNTED HORIZONTAL TAIL AT MACH NUMBERS FROM 0.60 TO 1.075

By Robert J. Ward and Joseph M. Hallissy, Jr.

SUMMARY

An investigation was conducted in the Langley 16-foot transonic tunnel and the 8-foot transonic pressure tunnel of a sweptback T-mounted horizontal tail with various modifications at Mach numbers from 0.60 to 1.075 and for wing angles of attack from -4° to 14°. The basic horizontal tail had an aspect ratio of 3.5, an NACA 63A009 airfoil section, and a sweep of the quarter-chord line of 40°. This horizontal tail was mounted on the sweptback vertical tail of a seaplane model designed for transonic speeds. Pressure, force, and hinge-moment data are presented on the basic horizontal tail, but no pressure data were obtained on the modifications. Some sideslip data are also presented.

A hinge-moment couple is shown to exist at zero tail loading because of interference of the vertical tail, bullet fairing, and fuselage base on the horizontal tail. Transonic stabilizer hinge moments several times greater than at subsonic speeds resulted from the shift of the aerodynamic center in the basic stabilizer. A thin delta tail eliminated interference effects and delayed but did not reduce the aerodynamic-center shift. Variation of the stabilizer hinge-moment level through use of elevator deflection, bullet-mounted flaps, or other camber-changing devices is shown to minimize the adverse effect of the aerodynamic-center shift.

INTRODUCTION

Among the design problems for large aircraft intended for flight at transonic or supersonic speeds are those associated with the horizontal tail. Because of the transonic aerodynamic-center shift, the stabilizer

is required to be a much more powerful trimming device for a transonic than for a subsonic airplane. This requirement, coupled with the large physical size of control area required, forces the use of a fully boosted all-movable tail. A particular problem is that of designing the actuator, which is necessarily large for such an airplane. Careful attention needs to be given to the tail hinge-moment characteristics if the actuator is to be capable of handling these moments for all flight conditions without being excessively large.

In spite of these rather obvious requirements, the amount of detailed loads information and analysis work which has been published for tails designed to be operated in the transonic speed range is limited. It is believed, therefore, that the results of recent wind-tunnel tests of a transonic seaplane model having a T-mounted horizontal tail will be of general interest. Tail-loads data were obtained, with particular emphasis on the basic-stabilizer hinge moments. The investigation was conducted with a view to providing hinge-moment relieving devices.

The test Mach number range was from 0.60 to 1.075, the wing angle-of-attack range was from -4° to 14°, and sideslip angles were $\pm 2^\circ$ and $\pm 5^\circ$. Pressure data and strain-gage data were obtained on the horizontal tail only and are reported herein.

SYMBOLS

b span, ft

$C_{b,t}$ $\dfrac{4 \times \text{Stabilizer bending moment}}{qS_t b_t}$

$\Delta C_{b,t}$ incremental stabilizer root-bending-moment coefficient, $(C_{b,t})_{right} - (C_{b,t})_{left}$

$C_{h,o}$ residual stabilizer hinge-moment coefficient, $C_{h,t}$ at $C_{N,t} = 0$

$\Delta C_{h,o}$ incremental residual stabilizer hinge-moment coefficient, $C_{h,o}$ of modification minus $C_{h,o}$ of basic stabilizer

$C_{h,t}$ stabilizer hinge-moment coefficient, $\dfrac{\text{Stabilizer hinge moment}}{qS_t c_t'}$

$\frac{\partial C_{h,t}}{\partial C_{N,t}}$ hinge-moment parameter at $C_{N,t} \approx 0$

C_m wing pitching-moment coefficient measured about 0.25c', $\frac{M_{c'/4}}{qS_w c'_w}$

ΔC_m C_m with tail on minus C_m with tail off taken at same angle of attack

$C_{N,t}$ stabilizer normal-force coefficient,

$$\frac{N}{qS_t} = \int_0^{1.0} c_{n,t}\left(\frac{c}{\bar{c}}\right)_t d\left(\frac{y}{b/2}\right)_t \quad \text{or} \quad -\Delta C_m\left(\frac{1}{\text{Tail volume}}\right)$$

C_p pressure coefficient, $\frac{p_l - p_\infty}{q}$

c local chord, ft

$c_{n,t}$ stabilizer section normal-force coefficient,

$$\frac{N \text{ per foot of span}}{qc_t} = \int_0^{1.0} (C_{p,l} - C_{p,u}) d\left(\frac{x}{c}\right)_t$$

$\bar{c}$ average chord, ft

c' mean aerodynamic chord, ft

i_t angle of tail incidence relative to wing root-chord plane (nose up, positive), deg

M Mach number

$M_{c'/4}$ pitching moment about wing c'/4, ft-lb

N horizontal-tail normal force, lb

p static pressure, lb/sq ft

q free-stream dynamic pressure, lb/sq ft

S	area, sq ft
t	maximum thickness, ft
x	chordwise distance, ft
y	spanwise distance, ft
α_w	angle of attack of wing root chord, deg
β	angle of sideslip, deg
δ_e	elevator deflection angle (trailing edge down, positive), deg

Subscripts:

∞	free stream
l	local or lower surface
u	upper
w	wing
t	horizontal tail

APPARATUS

Wind Tunnels

The investigation was conducted in the Langley 16-foot transonic tunnel and the 8-foot transonic pressure tunnel. The 16-foot transonic tunnel is a single-return octagonal slotted-throat wind tunnel and operates at approximately atmospheric total pressure. The maximum variation of average Mach number is about ±0.002 along the test-section center line in the vicinity of the model. Additional details of the test-section configuration and of the tunnel calibration are given in reference 1. The 8-foot transonic pressure tunnel has a square test section, with slots on the top and bottom only, and may be operated over a range of total pressures. The maximum variation of average Mach number is about ±0.007 along the test-section center line in the vicinity of the model.

Model

A sketch and a photograph of the high-speed seaplane model used in the investigation are shown in figure 1. Table I gives the dimensions of the basic model together with the dimensions of the various stabilizer and bullet configurations. Sketches of the tail configurations are presented in figure 2. A swept stabilizer and a bullet fairing are included in the basic tail configuration. Minor modifications to the basic tail were bullet-mounted flaps, a bullet-mounted spoiler, and a revised bullet. The major modification tested was a thin delta tail of approximately the same span and projected area as the basic tail. A minor nacelle modification was included with the revised bullet in the final test series.

Model Support System and Instrumentation

The same model and balance were used in both tunnels with similar sting support systems. The model was mounted on a six-component strain-gage balance, and wire strain gages were used to measure hinge moments. In the 16-foot transonic tunnel the support system, described in reference 2, rotated the model about the quarter-chord point of the wing mean aerodynamic chord, while in the 8-foot transonic pressure tunnel the center of rotation was 40 inches aft of the quarter-chord reference point.

TESTS

This investigation was conducted under four test programs as given in table II. The Reynolds number is based on a stabilizer mean aerodynamic chord of 4.834 inches. Transition, when used, was placed on the wing and on both the horizontal and the vertical tail. The effects on the stabilizer hinge-moment characteristics of transition and of the bullet and nacelle modifications in test series 4 proved to be negligible.

DATA REDUCTION, ACCURACY, AND CORRECTIONS

Data-Reduction Methods

A punched-card system was used extensively to facilitate data reduction. Pressure data were recorded with manometer-board cameras and then transferred to cards. Airplane pitching-moment data were obtained with an electrical strain-gage balance; electrical strain gages were also used to obtain stabilizer hinge moments. These strain gages read out on self-balancing potentiometers connected to digital converters, and readings

were recorded on cards and on a tabulator. Section normal-force and hinge-moment coefficients were integrated numerically from the individual pressure coefficients.

Accuracy and Corrections

Correction was made for an upflow angle of 0.17° in the 16-foot transonic tunnel and for a downflow angle of 0.1° in the 8-foot transonic pressure tunnel. No corrections have been made for tunnel-wall or other interference effects. For the 16-foot transonic tunnel, past experience has shown that these effects are negligible up to a Mach number of 1.03 for models of the size used in this investigation. Above this Mach number, as shown in reference 3, wall-reflected disturbances will affect the accuracy of the data, particularly at high angles of attack. The model used in these tests is about three times as large as those normally used in the 8-foot transonic pressure tunnel, and the test results from test series 3 could, therefore, be subject to error, particularly at the higher speeds. However, it is believed that the incremental effects used in this study, such as the incremental effect of elevator deflection on stabilizer hinge moments, would not be significantly in error.

The accuracy of angle settings and of pressure, force, and moment coefficients is believed to be within the limits shown in the following table. Coefficient accuracy is based on instrument error at a Mach number of 0.80 and on repeatability of data.

Accuracy of -	16-foot transonic tunnel	8-foot transonic pressure tunnel
α_w, deg	±0.1	±0.1
δ_e, deg	±0.2	±0.2
i_t, deg	±0.2	±0.2
$C_{N,t}$ (pressure)	±0.01	
$C_{N,t}$ (strain gage)	±0.02	
$C_{h,t}$ (pressure)	±0.007	
$C_{h,t}$ (strain gage)	±0.002	±0.002

RESULTS AND DISCUSSION

Characteristics of Basic Stabilizer

Basic-stabilizer section pressure distributions are presented in figure 3. It will be noted that the vertical tail, bullet fairing, and fuselage base have a marked effect on the lower-surface pressure distribution, particularly at the inboard station for Mach numbers of 0.95 and 1.00. The lower-surface pressures become more negative than the upper-surface pressures near the leading edge and more positive near the trailing edge and, thus, contribute a negative increment to the section moment. This negative hinge-moment increment at zero tail loading produces a residual stabilizer hinge moment which varies with Mach number and reaches a maximum at approximately $M = 1.00$. The section pressure distribution also changes from a triangular subsonic distribution at $M = 1.00$ to a rectangular transonic distribution at $M = 1.075$ (fig. 3(b)); this behavior indicates a rearward aerodynamic-center shift.

The basic-stabilizer spanwise load distribution (fig. 4) indicates uniform downwash distribution in the vicinity of the stabilizer because the section load becomes zero for all sections at about the same angle of attack. Elevator deflection is shown to produce a load increment which decreases slightly with an increase in Mach number. The integrated basic-stabilizer normal loading (fig. 5) shows generally linear characteristics with angle of attack and only minor changes in slope with an increase in Mach number. Elevator deflection shifted the stabilizer load level but did not have a significant effect on the normal-force slope.

Basic-stabilizer hinge-moment coefficients were computed from both strain-gage and pressure measurements and are presented in figure 6. A comparison of strain-gage and pressure data (fig. 6(a)) shows general agreement, although the pressure data are subject to scatter. Consequently, strain-gage data are used when presenting stabilizer hinge-moment results in all subsequent plots. The rearward shift of the aerodynamic center at transonic speeds is evident as an increased slope of the curves for $C_{h,t}$ plotted against $C_{N,t}$ with an increase in Mach number. Elevator deflection has only a minor effect on the aerodynamic-center shift as taken at $C_{N,t}$ approximately equal to zero. (See fig. 7.) However, elevator deflection does have a noticeable effect on the stabilizer hinge-moment level (fig. 8). Negative elevator deflection shifts the hinge-moment level in the positive direction, as does a more negative stabilizer loading.

Results from another test series in which data were obtained at much smaller increments in Mach number are presented in figure 9. This figure indicates that the rearward aerodynamic-center shift is quite abrupt and that the shift occurs between Mach numbers of 1.01 and 1.02. A comparison of these data with the data of figure 6(a) shows some discrepancies which are representative of the sensitivity of the hinge moments to small differences in M, α_w, i_t, and δ_e.

Stabilizer incidence is shown to have little effect on the basic-stabilizer hinge-moment characteristics up to a wing angle of attack of 8°. (See fig. 10.) This fact is attributed to the high stabilizer location placing the tail in a uniform downwash field.

The effect of sideslip on basic-stabilizer characteristics is shown in figure 11 for 2° and 5° of sideslip. Asymmetric stabilizer loading resulting from sideslip (fig. 11(a)) produces an incremental stabilizer root-bending-moment coefficient that is relatively independent of Mach number, elevator deflection, or angle of attack (fig. 11(b)). Furthermore, the stabilizer hinge-moment characteristics are unaffected by sideslip (fig. 11(c)).

Minimization of Tail Hinge Moments

As mentioned previously, careful attention needs to be given to the tail hinge-moment characteristics for large airplanes if the actuator is to be capable of handling the hinge moments for all flight conditions without being excessively large. For the present model an analysis of these hinge moments is greatly simplified by the characteristic already pointed out in figure 10; that is, the high horizontal-tail position results in the hinge moment at a given Mach number being dependent only on tail normal force and independent of tail incidence.

Figure 10 also indicates that the stabilizer hinge-line location was chosen to coincide approximately with the low-speed aerodynamic center. This hinge-line choice, plus the fact that the hinge moment for zero tail load $C_{h,o}$ is small for speeds up to M = 0.80, means that in this speed range the tail hinge-moment coefficient is small no matter what the tail normal force is. As speed is increased, however, two things occur which can cause greatly increased hinge moments. First, the slope of the curve for hinge-moment parameter plotted against Mach number changes to a negative value (fig. 12, basic tail); that is, the aerodynamic center shifts rearward from the hinge line as the speed is increased through the transonic range. Second, the hinge moment for zero lift (residual stabilizer hinge moment $C_{h,o}$) varies, as shown in figure 13, initially in the negative direction for high subsonic speed

and then back toward zero as the speed is increased to supersonic values. Thus, depending on the tail normal-force requirements, the resulting hinge moments, even for 1 g trimmed flight, may exhibit a large and unusual variation with Mach number.

Possible approaches for reducing these tail hinge moments include: (a) elimination or reduction of the transonic aerodynamic-center shift, (b) change of hinge-line location with Mach number to compensate for the aerodynamic-center shift, and (c) adjustment of $C_{h,o}$ to provide reduced hinge moments at the required stabilizer normal force. Of these, approach (b) is not discussed herein, since such a change has more the nature of an engineering feasibility problem rather than an aerodynamic problem.

With regard to approach (a) (eliminating or reducing the transonic aerodynamic-center shift), it is believed certain that minor geometry modifications cannot affect this basic phenomenon. A number of such modifications were made during this investigation, with very little effect on the aerodynamic-center shift; for example, a bullet modification (fig. 2(a) and table I) had no noticeable effect on any of the hinge-moment characteristics. Major geometry changes can, perhaps, do more. For instance, figure 12 indicates that for a $\frac{t}{c} = 0.05$ delta plan-form tail of area equal to that of the original tail, the aerodynamic-center shift was delayed to a Mach number of 1.0. At that point, however, the aerodynamic center moved very rapidly rearward, and the total shift was as great as for the basic tail. This behavior is considered representative of any feasible geometry change; some improvement is possible, especially as to the Mach number where the aerodynamic-center shift occurs, but the total reduction in aerodynamic-center shift possible will not be great.

The thin delta tail was also effective in eliminating interference effects on the stabilizer (fig. 13). Elimination of interference would be advantageous for an aircraft that trims near zero tail load. However, for an aircraft that trims with a negative tail load, figure 10 shows that a negative $C_{h,o}$ would be desirable at high Mach numbers where the aerodynamic center has shifted rearward. This characteristic can be provided artificially by controlling $C_{h,o}$ through a physical camber change programed with Mach number. Any manner of altering the effective stabilizer camber may be used. For a tail equipped with an elevator intended for use at low speed, as in the present case, the elevator, instead of being locked at transonic speeds, may be programed with Mach number to obtain the desired $C_{h,o}$ variation. Bullet-mounted flaps or a spoiler are also effective in varying $C_{h,o}$. Figure 14 shows

increments in stabilizer hinge-moment coefficient which are obtained by deflection of any one of these controls. These increments are taken at a tail normal load of zero.

CONCLUSIONS

An investigation has been made of the load and hinge-moment characteristics of a swept T-mounted horizontal tail with various modifications. This horizontal tail was mounted on the sweptback vertical tail of a seaplane model designed for transonic speeds. Stabilizer pressure distributions, normal force, and hinge moments are presented for a Mach number range of 0.60 to 1.075 and for a wing angle-of-attack range of -4° to 14°. Some sideslip data are also presented. The results of the investigation indicate the following conclusions:

1. Interference of the vertical tail, bullet fairing, and fuselage base on the horizontal tail produces a residual stabilizer hinge moment, a hinge moment at zero tail loading, which varies with Mach number and reaches a maximum at a Mach number of approximately 1.00.

2. The rearward shift of the center of pressure at transonic speeds results in stabilizer hinge moments several times greater than at subsonic speeds, depending on the tail load required for trim.

3. A thin delta tail may be employed to eliminate the interference effects on the stabilizer, but such a tail is effective only in delaying the transonic aerodynamic-center shift.

4. The effect of the transonic aerodynamic-center shift can be minimized through variation of the hinge-moment level. Elevator deflection, bullet-mounted flaps, or other devices capable of altering the effective stabilizer camber may be employed to vary the hinge-moment level without affecting the linearity or slope of the curve for hinge-moment characteristics.

Langley Research Center,
National Aeronautics and Space Administration,
Langley Field, Va., June 11, 1959.

REFERENCES

1. Ward, Vernon G., Whitcomb, Charles F., and Pearson, Merwin D.: Air-Flow and Power Characteristics of the Langley 16-Foot Transonic Tunnel With Slotted Test Section. NACA RM L52E01, 1952.

2. Hallissy, Joseph M., and Bowman, Donald R.: Transonic Characteristics of a 45° Sweptback Wing-Fuselage Combination - Effect of Longitudinal Wing Position and Division of Wing and Fuselage Forces and Moments. NACA FM L52K04, 1953.

3. Whitcomb, Charles F., and Osborne, Robert S.: An Experimental Investigation of Boundary Interference on Force and Moment Characteristics of Lifting Models in the Langley 16- and 8-Foot Transonic Tunnels. NACA RM L52L29, 1953.

TABLE I

GEOMETRIC CHARACTERISTICS OF MODEL CONFIGURATIONS

[Wing thickness distribution varies linearly from $\frac{t}{c} = 0.11$ at root to $\frac{t}{c} = 0.08$ at tip, and wing incidence varies linearly from 3.0° at root to -2.0° at tip. Stabilizer hinge line was located 66.38 inches aft of model nose for all configurations.]

	Wing	Vertical tail	Basic horizontal tail	Delta horizontal tail
Airfoil section	NACA 63A3XX	NACA 63A010	NACA 63A009	Modified hexagon with 0.05 $\frac{t}{c}$
Area, projected, sq ft	3.852	0.433	0.5214	0.520
Span, projected, in.	54.0	7.884	16.20	16.18
Chord, in. -				
Root	15.411	10.152	6.30	8.43
Tip	5.133	5.67	2.97	0.83
Mean aerodynamic chord, in.	11.129	8.123	4.831	5.67
c'/4 location aft of nose, in.	28.77	59.901	66.26	65.96
Taper ratio	0.333	0.56	0.4741	0.0984
Aspect ratio	5.26	1.00	3.50	3.50
Incidence at root chord, deg	3		Variable	Variable
Twist, deg	-5		0	0
Dihedral, deg	-1.66		15	0
Sweepback, c/4, deg	40	45	40	35.18
Tail length ($c'_w/4$ to $c'_t/4$ along wing root-chord plane), in.			36.95	36.65
Tail volume, $\frac{S_t l_t}{S_t c'_w}$			0.449	0.445

	Used with basic stabilizer		Used with delta tail
	Original	Revised	
Bullet fairings:			
Length, in.	12.053	12.053	10.70
Frontal area, sq ft	0.0125	0.0187	0.0172
Fineness ratio, $\frac{\text{Bullet length}}{\sqrt{\frac{4}{\pi}(\text{Frontal area})}}$	7.97	6.52	6.04
Nose location (aft of model nose), in.	59.29	59.29	62.07
Bullet-mounted flaps for basic tail:			
Frontal area, sq ft	0.00338		
Location aft of stabilizer hinge line, in.	2.27		
Bullet-mounted spoiler for basic tail:			
Frontal area, sq ft	0.00623		
Location aft of stabilizer hinge line, in.	0		
Height, inboard section, in.	0.25		
Height, outboard sections, in.	0.20		

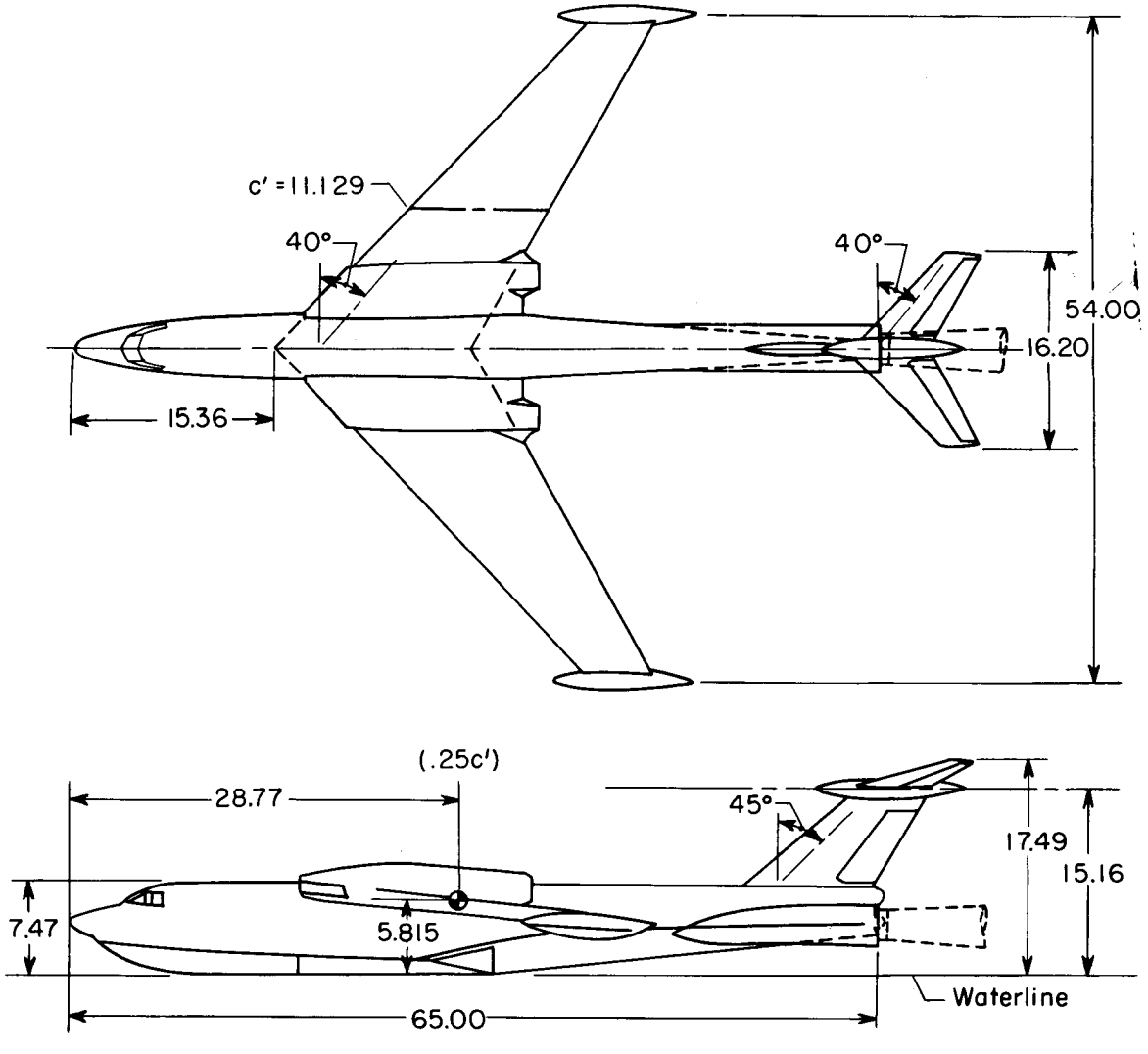

(a) Sketch of model. All linear dimensions are in inches.

Figure 1.- General arrangement of model.

TABLE II

TEST PROGRAM

	Test series 1	Test series 2	Test series 3	Test series 4
Tunnel	16-foot transonic tunnel	16-foot transonic tunnel	8-foot transonic pressure tunnel	16-foot transonic pressure tunnel
Mach number	0.80 to 1.075	0.60 to 1.075	0.80 to 1.10	0.60 to 1.03
Wing angle of attack, deg	-4 to 8	-2 to 10	-2 to 14	0 to 14
Sideslip angle, deg	±2, 0, ±5	0	0	0
Reynolds number	1.2×10^6 to 1.6×10^6	1.2×10^6 to 1.6×10^6	0.49×10^6 to 0.66×10^6	1.2×10^6 to 1.6×10^6
Model	Basic	Basic, thin delta tail, and basic with bullet-mounted flap	Basic and basic with bullet-mounted spoiler	Revised bullet and nacelles
Transition No. 120 carborundum grains	None	None	1/8-inch-wide strip at 0.10c	From 0.02c to 0.11c
Tail incidence, deg	-3	-1, -3, -5	-3, -5	+1, 0, -3, -5
Elevator deflection, deg	0, -4, -7	0	+2, 0, -2	0
Tail hinge-moment data	Pressure, strain gage	Strain gage	Strain gage	Strain gage

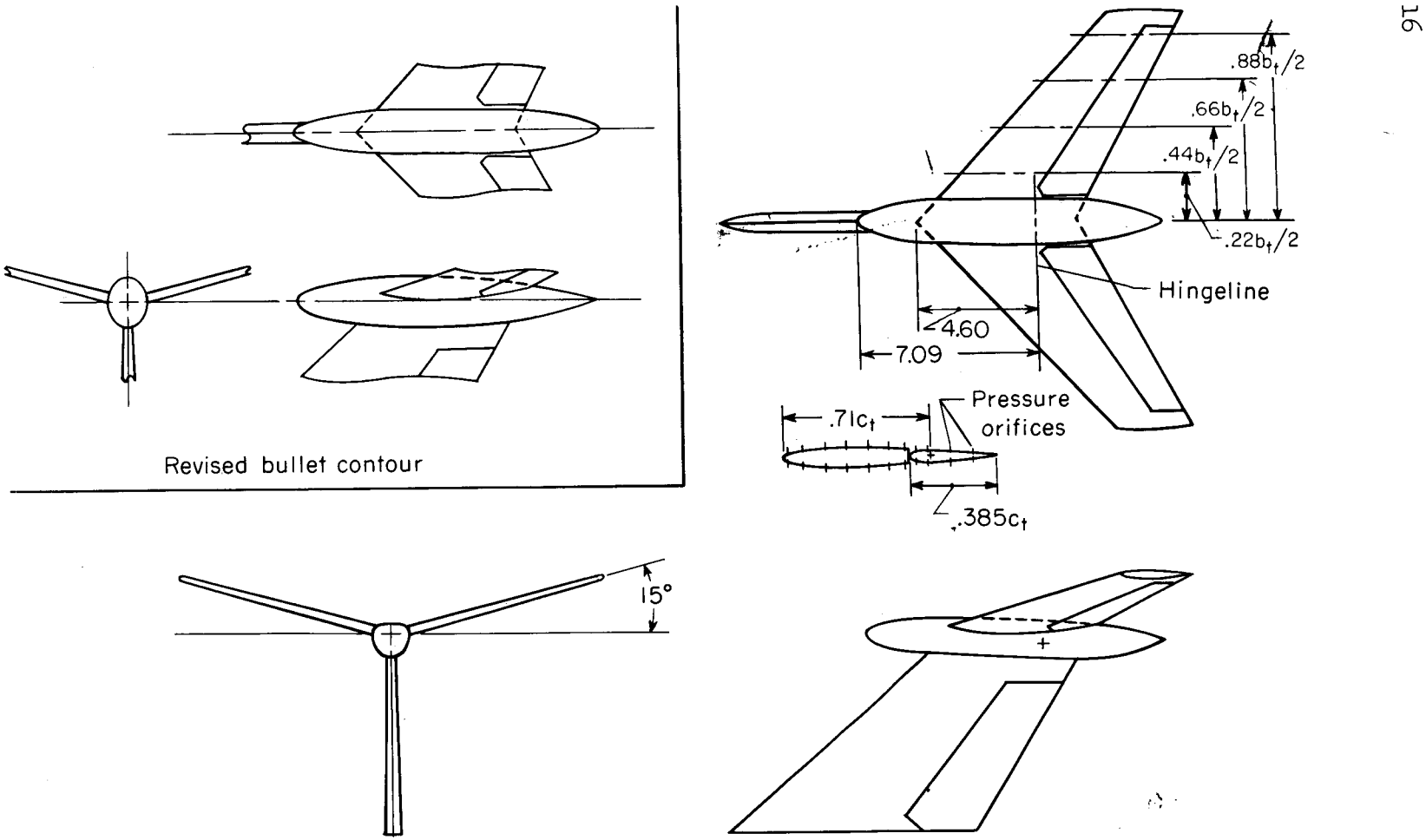

(a) Sketch of basic tail showing pressure-orifice and hinge-line locations and with original and revised bullets.

Figure 2.- Tail configurations. All linear dimensions are in inches.

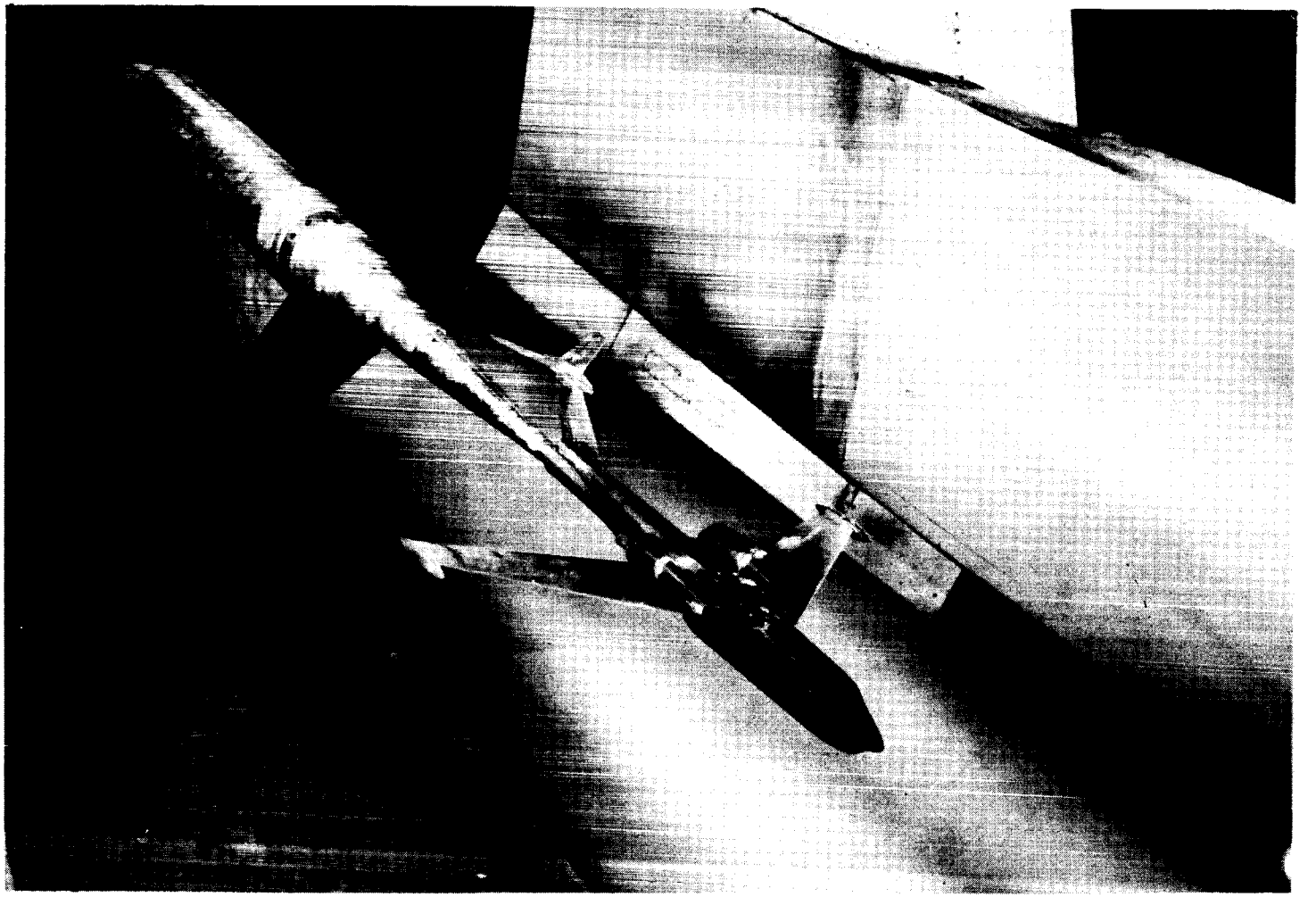

L-83542.1

(b) Three-quarter front view of model installed in Langley 16-foot transonic tunnel.

Figure 1.- Concluded.

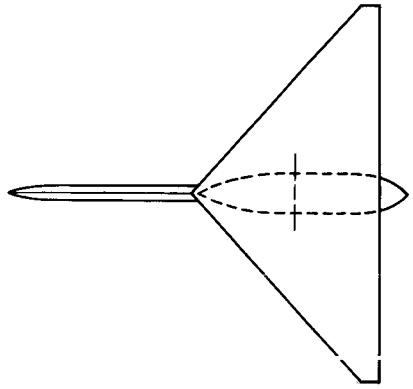

Thin (t/c = 0.05) delta tail

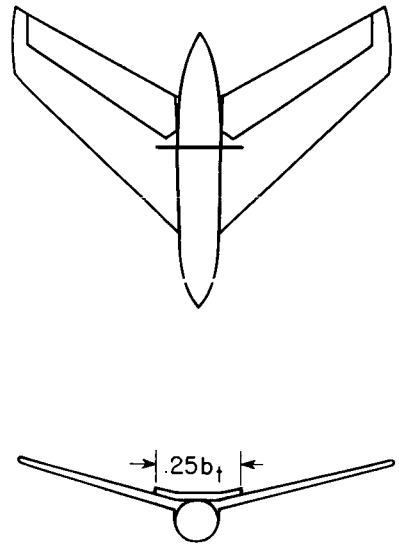

Bullet-mounted spoiler
on basic H.T.

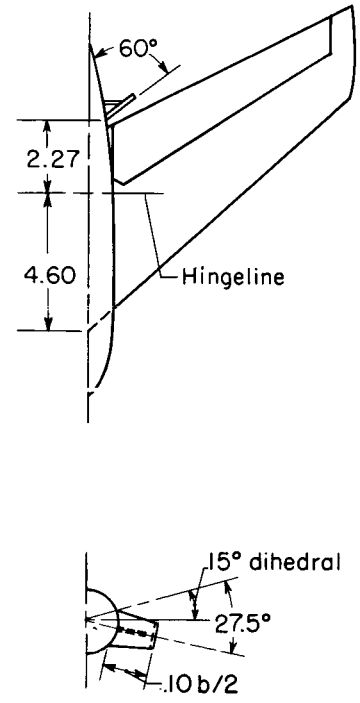

Bullet-mounted flap
on basic H.T.

(b) Modifications to basic tail.

Figure 2.- Concluded.

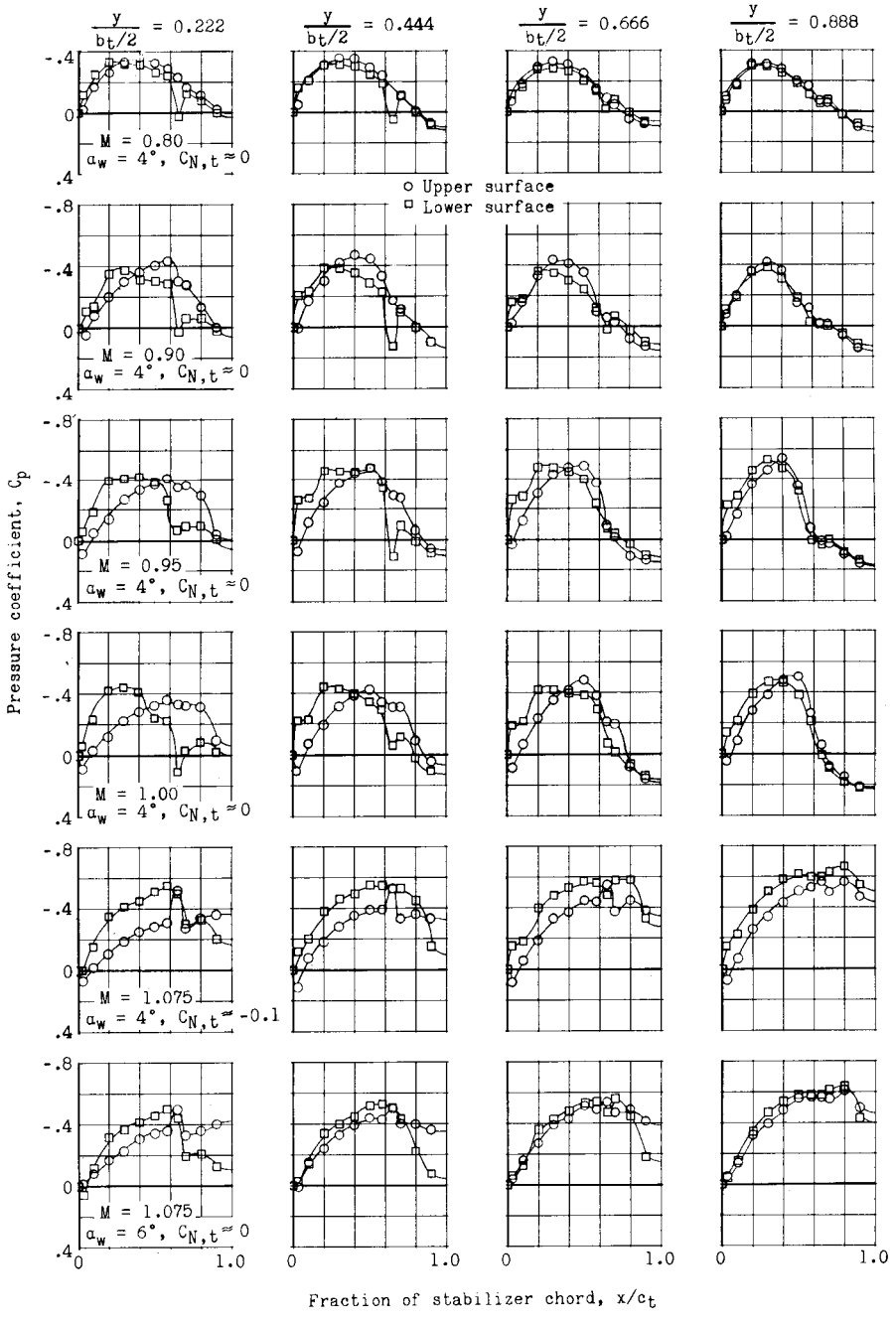

(a) Near-zero stabilizer lift.

Figure 3.- Basic-stabilizer chordwise load distribution for $i_t = -3^\circ$ and $\delta_e = 0^\circ$.

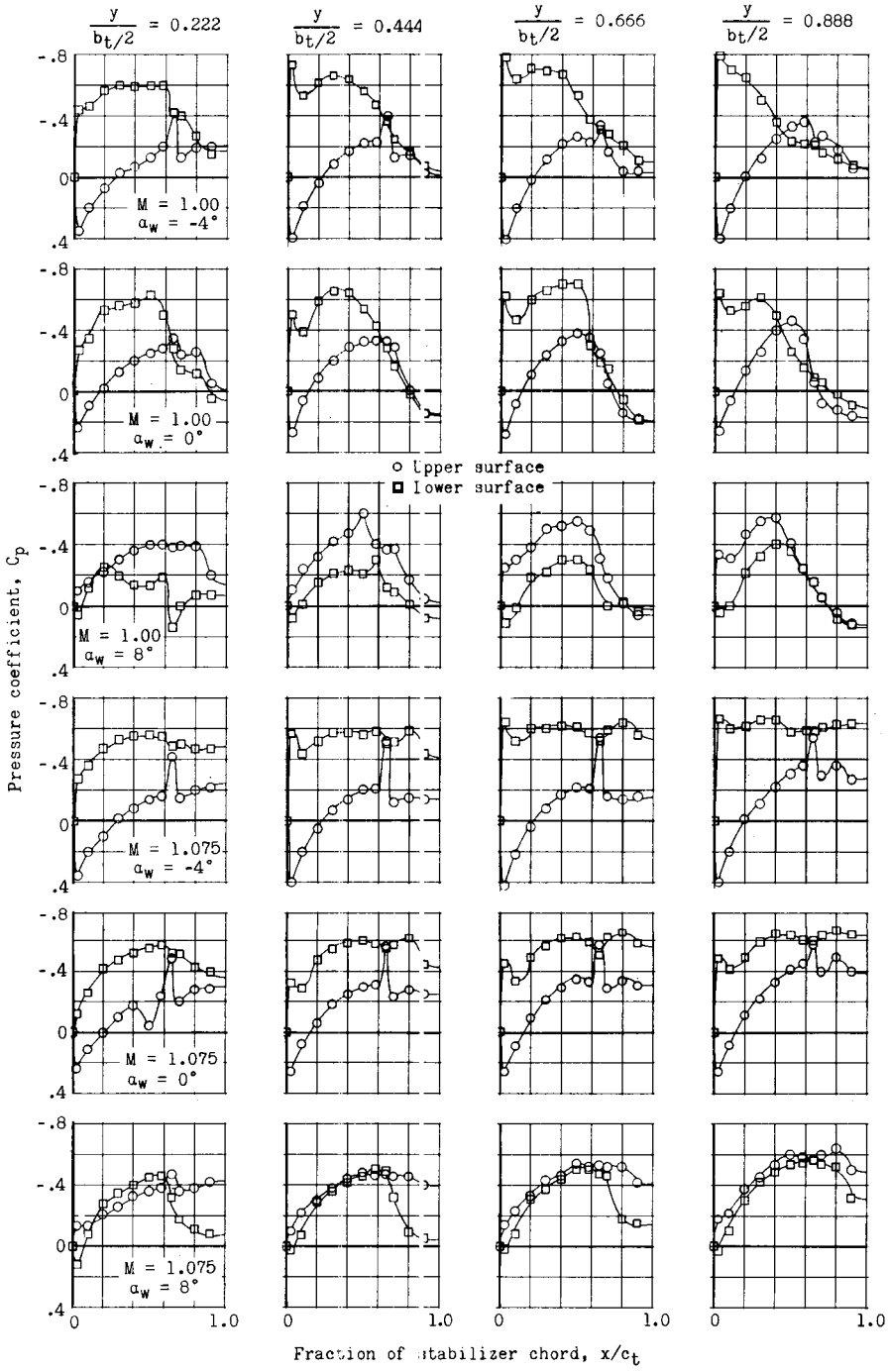

(b) Effect of angle of attack at M = 1.00 and M = 1.075.

Figure 3.- Concluded.

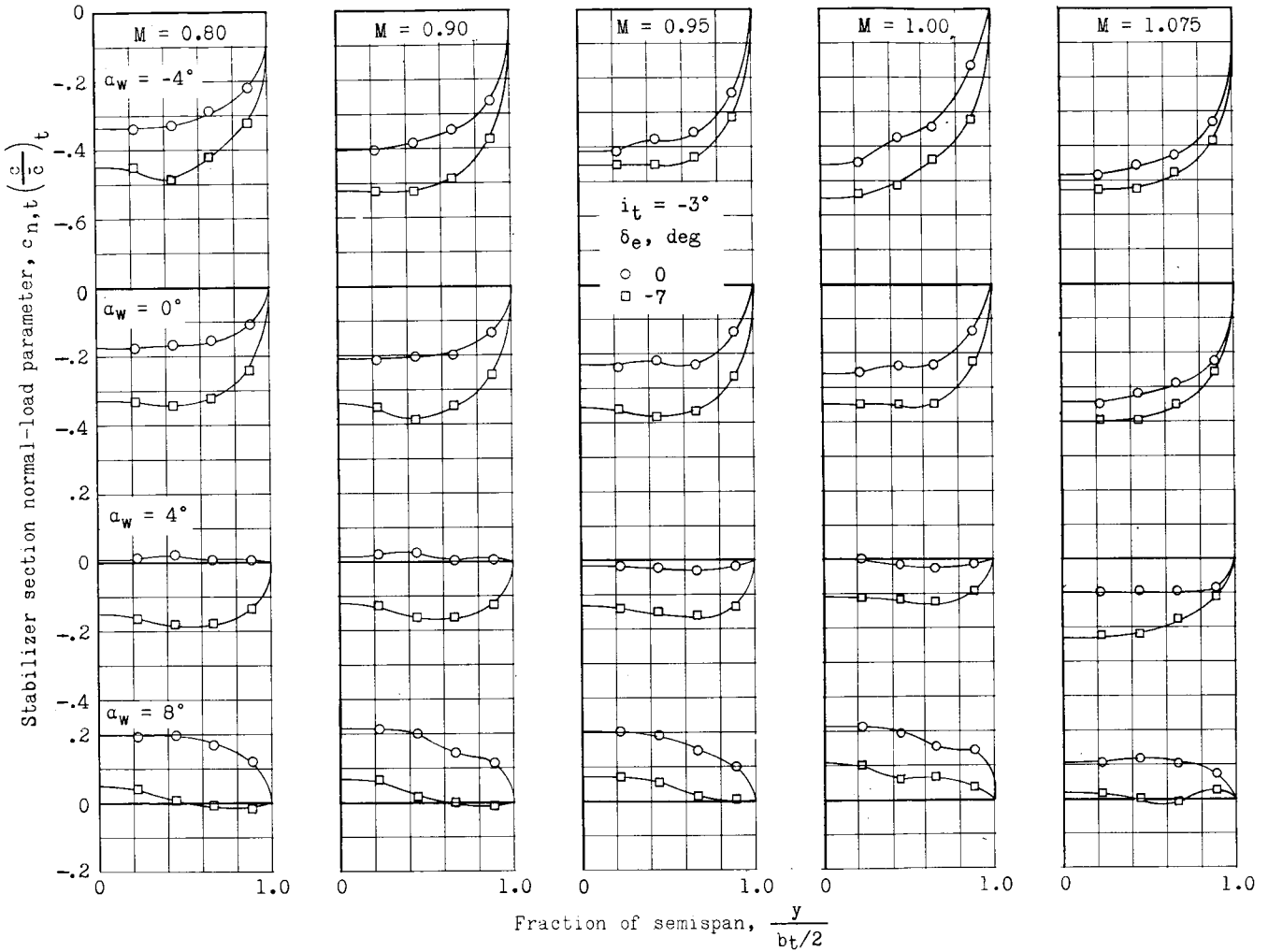

Figure 4.- Basic-stabilizer spanwise load distribution for $i_t = -3^\circ$ and for $\delta_e = 0^\circ$ and $\delta_e = -7^\circ$.

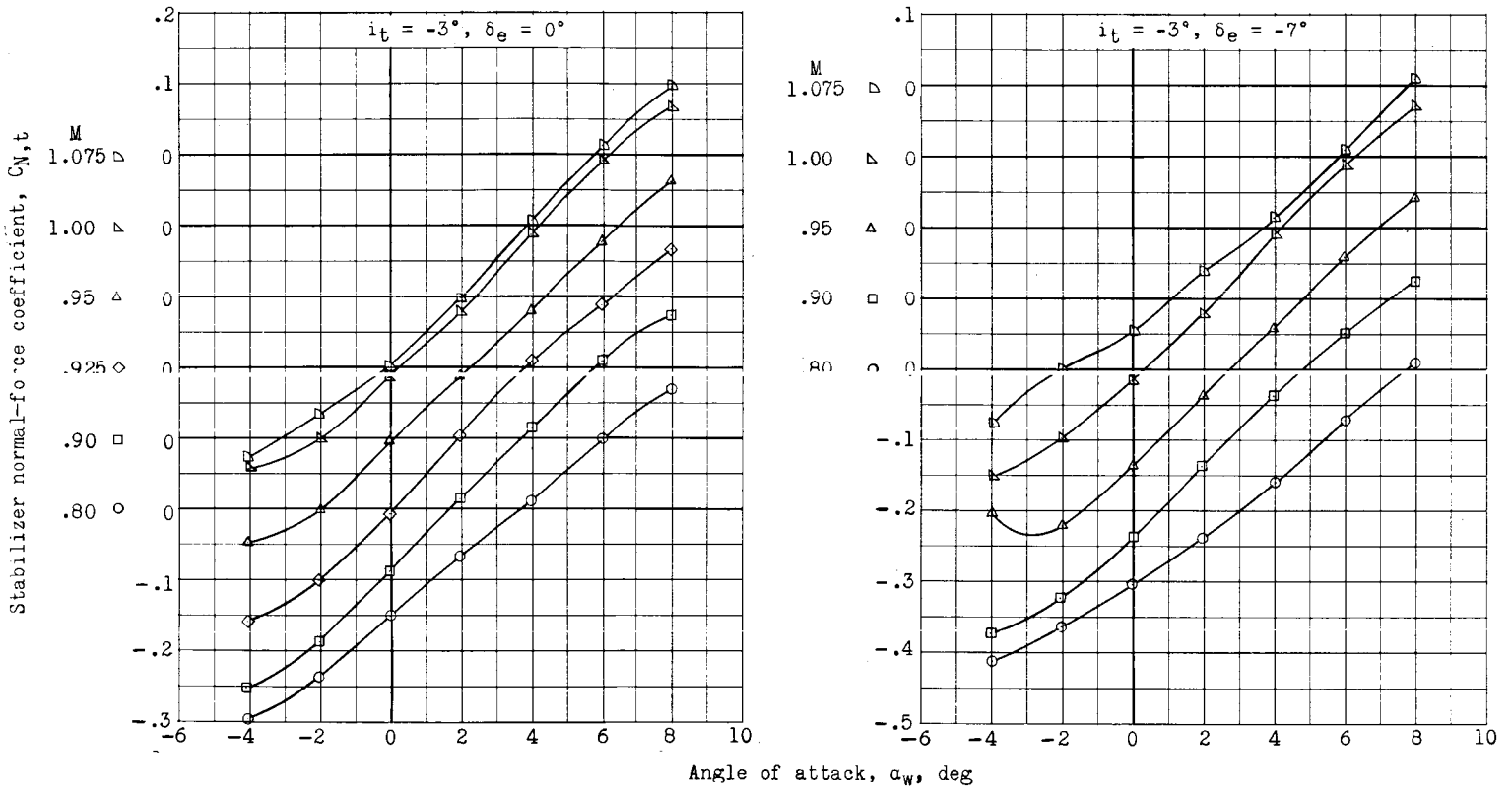

Figure 5.- Basic-stabilizer normal-force characteristics.

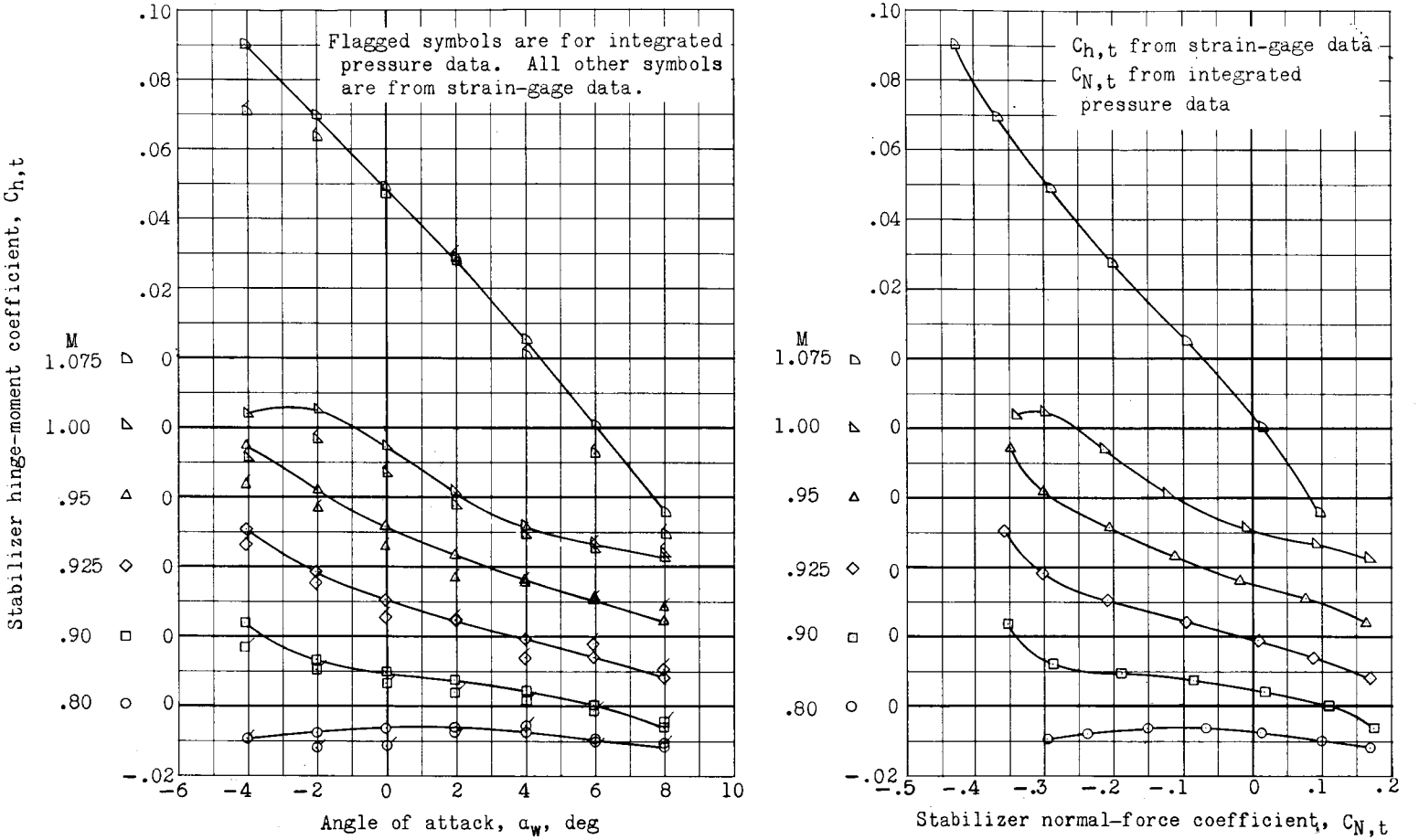

(a) Characteristics for $i_t = -3^\circ$ and $\delta_e = 0^\circ$.

Figure 6.- Basic-stabilizer hinge-moment characteristics.

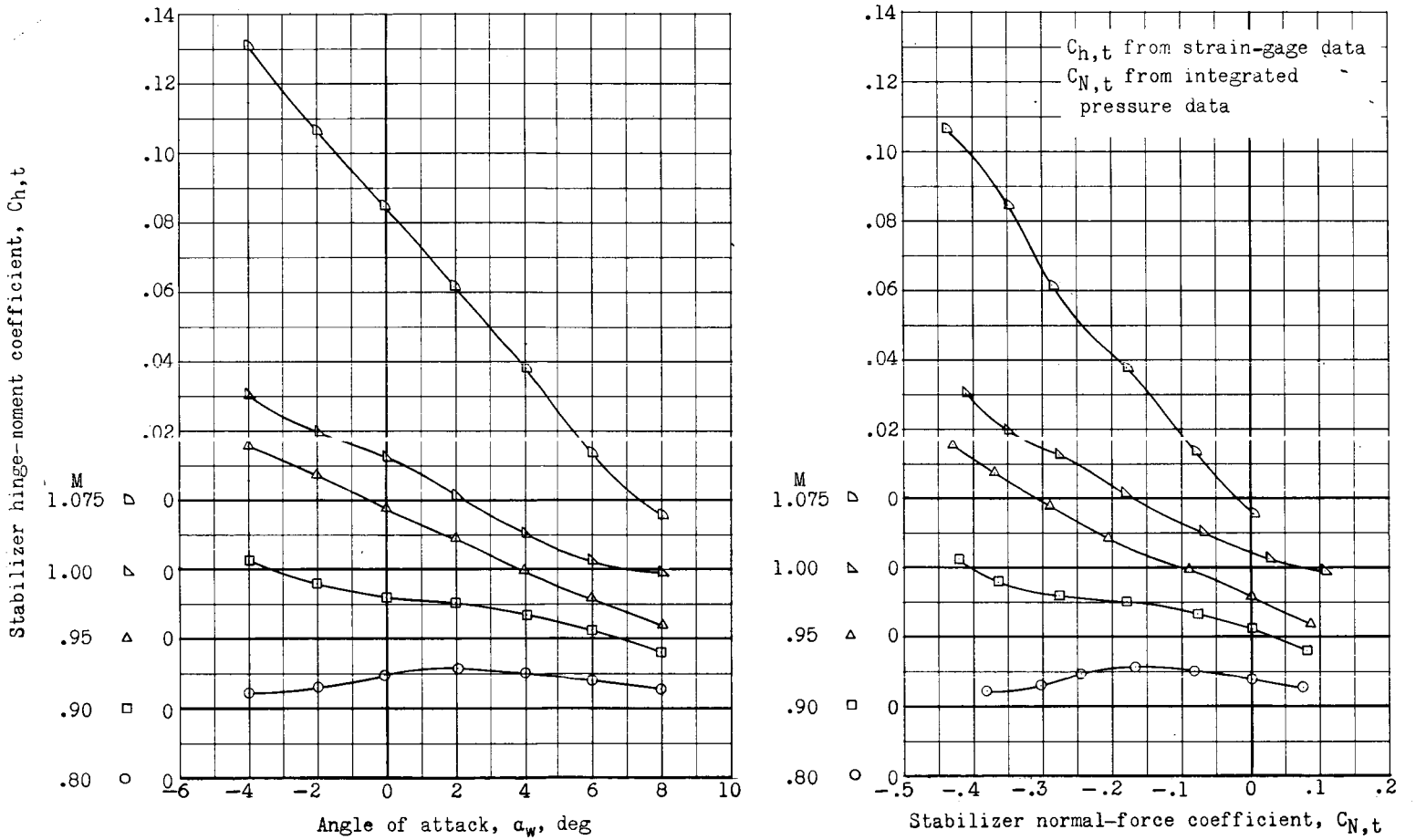

(b) Characteristics for $i_t = -3^\circ$ and $\delta_e = -4^\circ$.

Figure 6.- Continued.

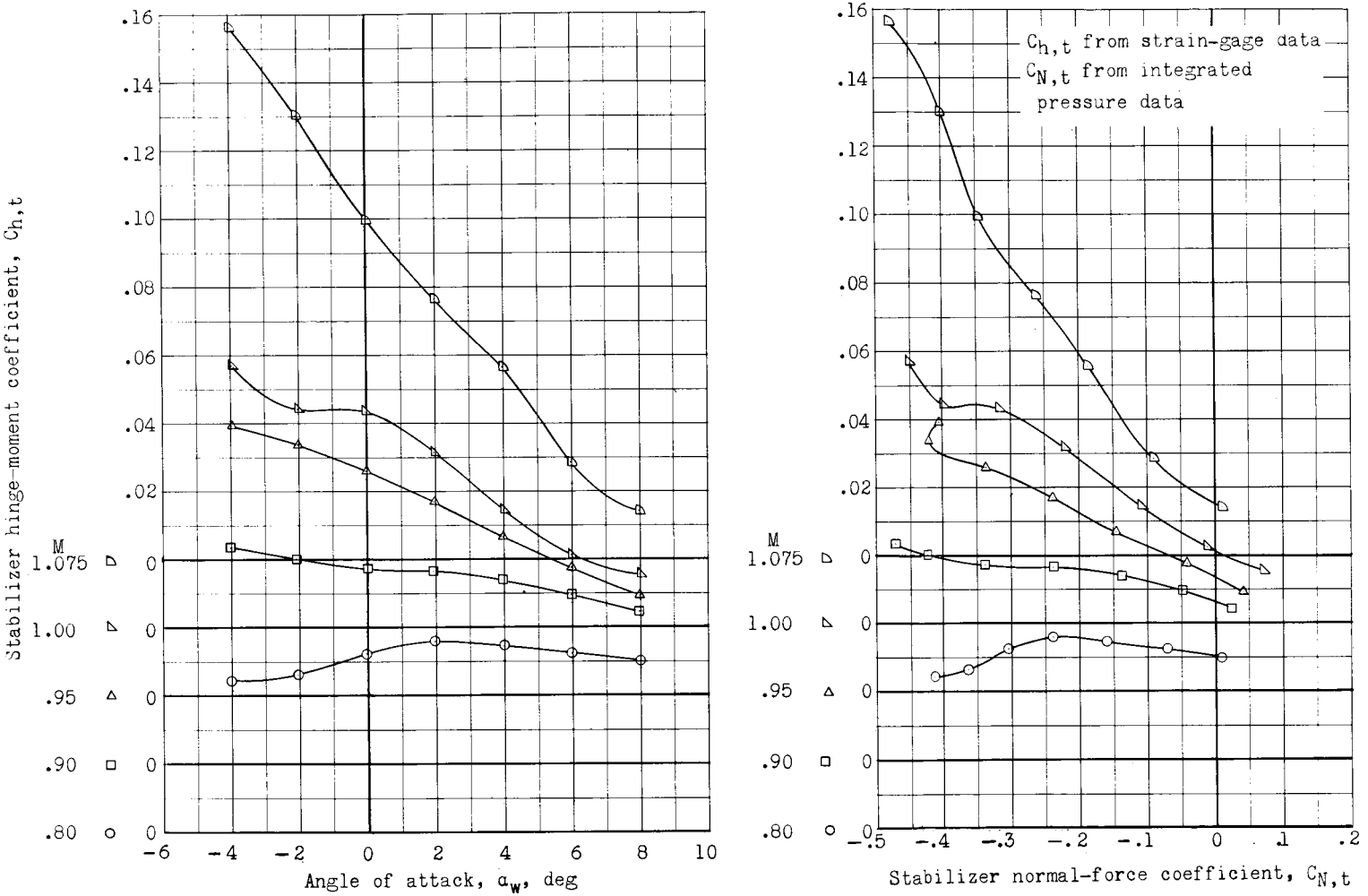

(c) Characteristics for $i_t = -3^\circ$ and $\delta_e = -7^\circ$.

Figure 6.- Concluded.

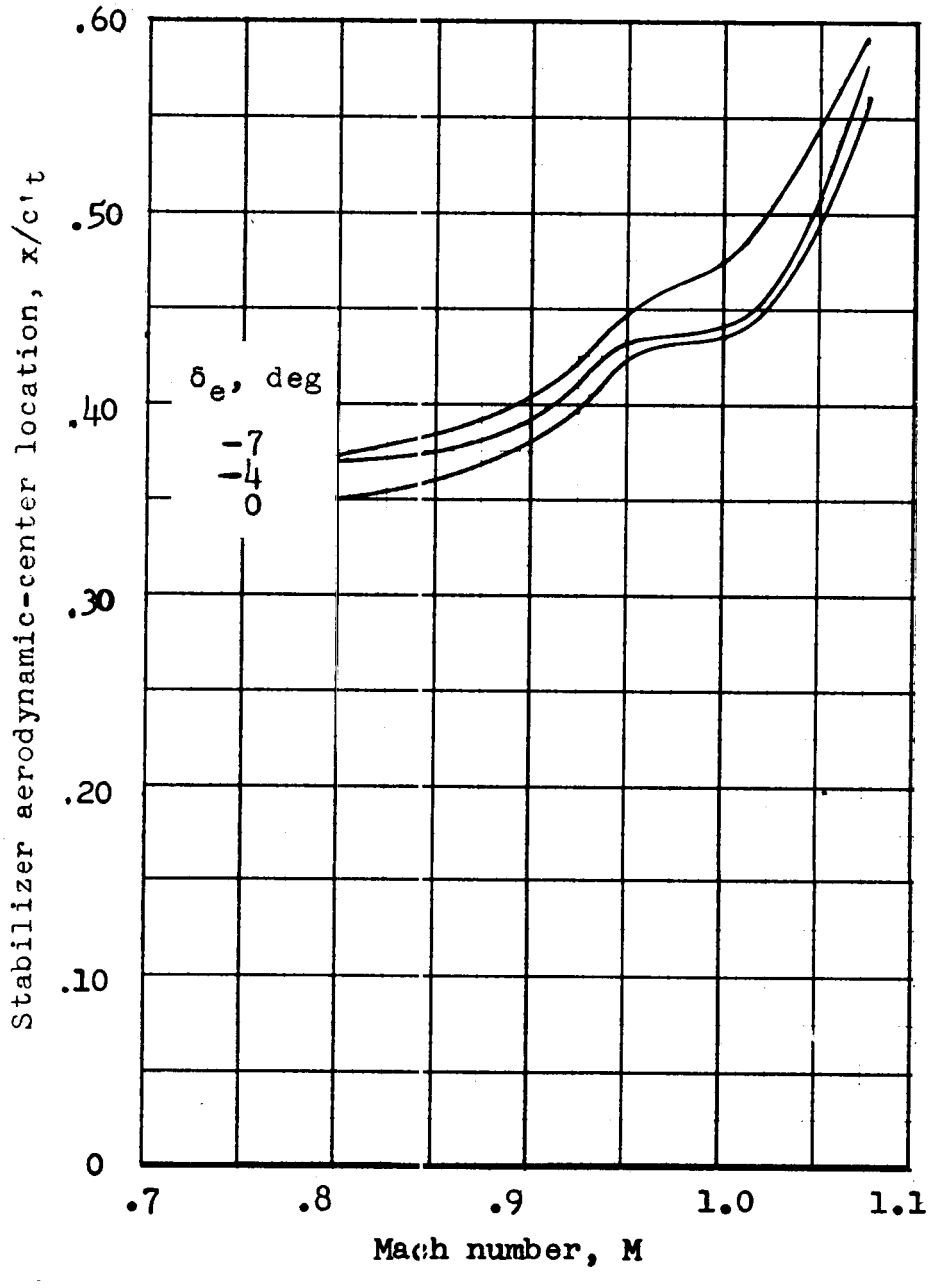

Figure 7.- Effect of Mach number on basic-stabilizer aerodynamic-center location. $C_{N,t} \approx 0$.

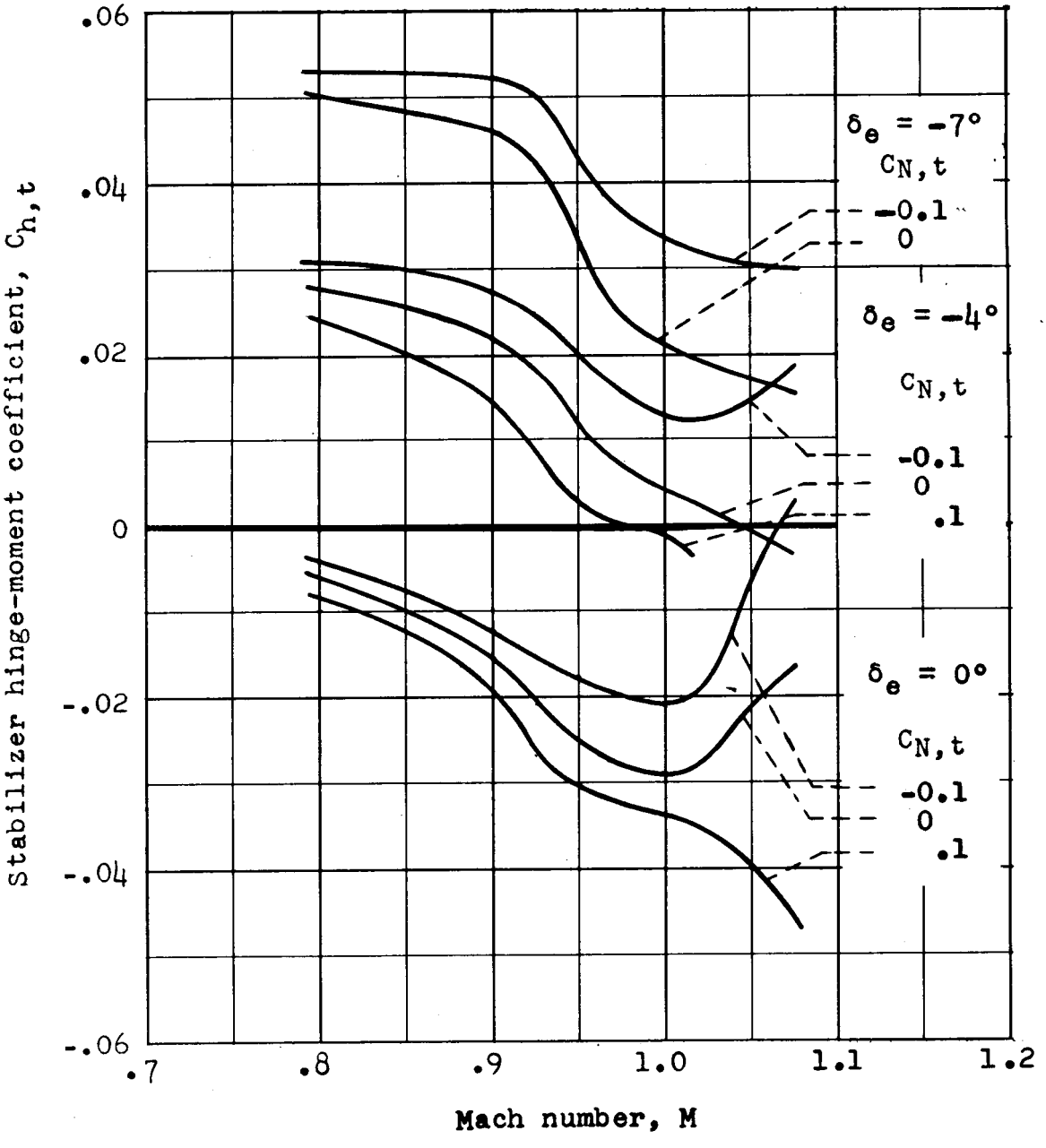

Figure 8.- Effect of Mach number on basic-stabilizer hinge-moment coefficient.

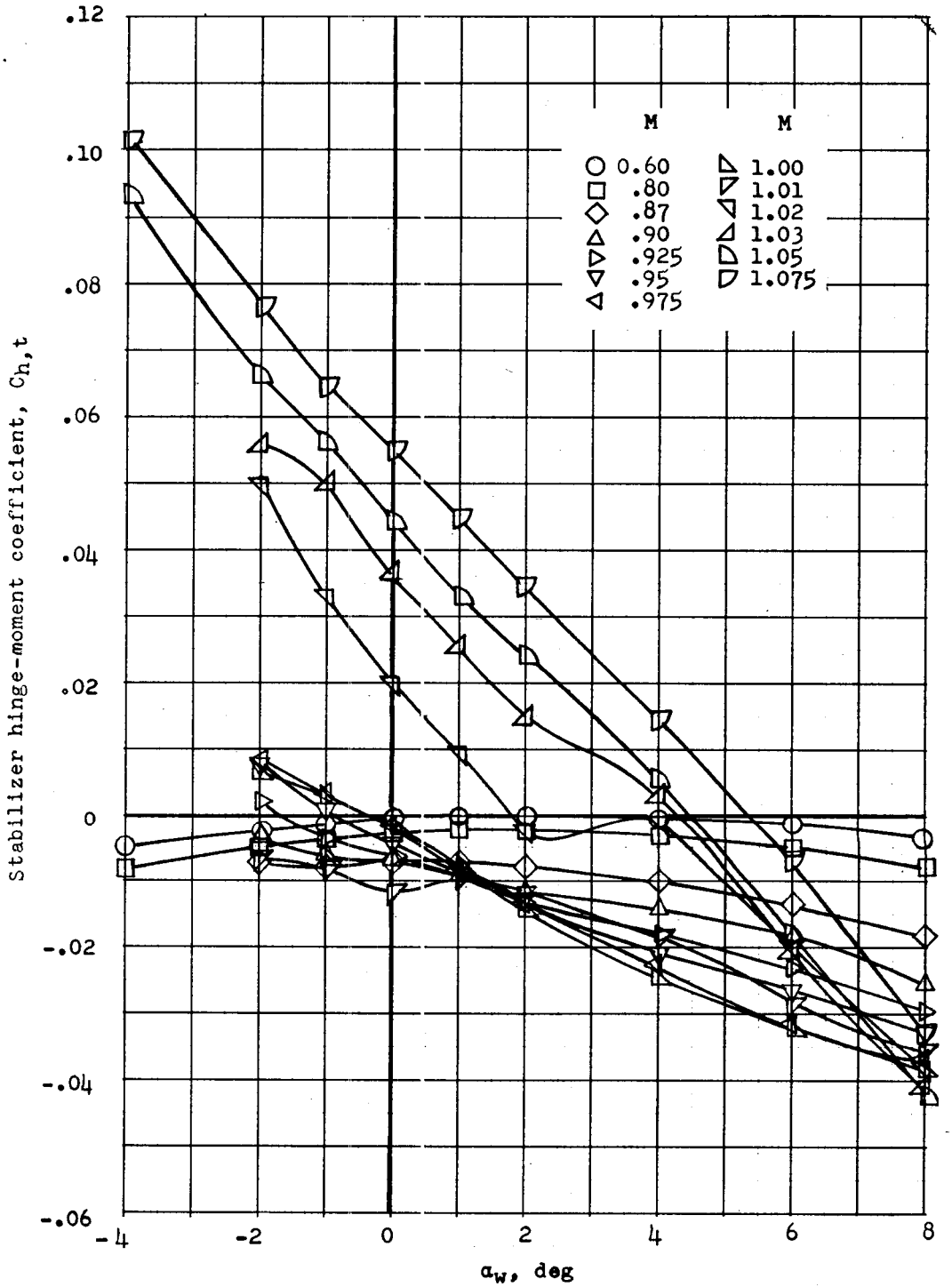

Figure 9.- Basic-stabilizer hinge-moment characteristics for $i_t = -3^\circ$ and $\delta_e = 0^\circ$.

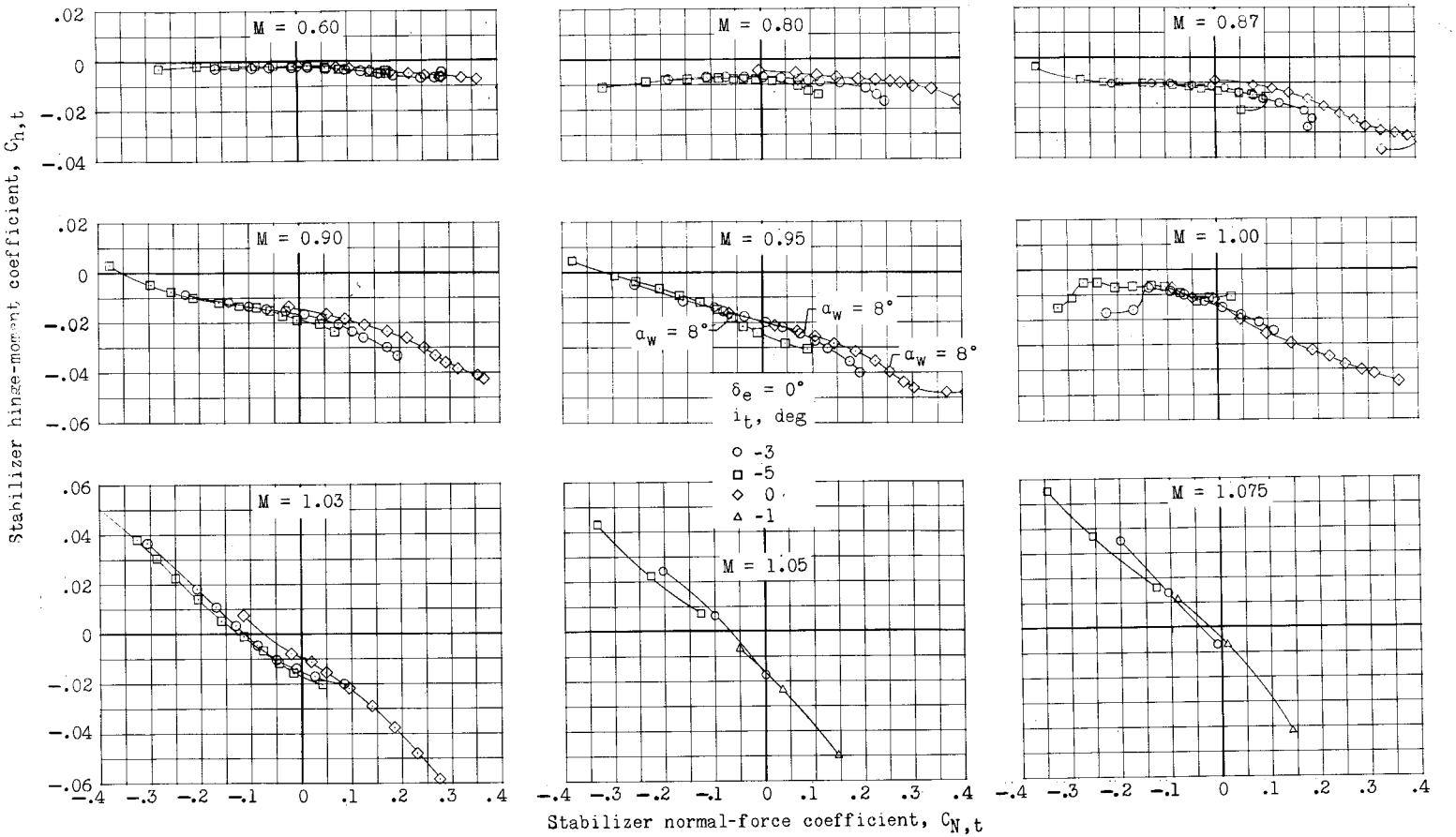

Figure 10.- Effect of stabilizer incidence on basic-stabilizer hinge-moment characteristics.

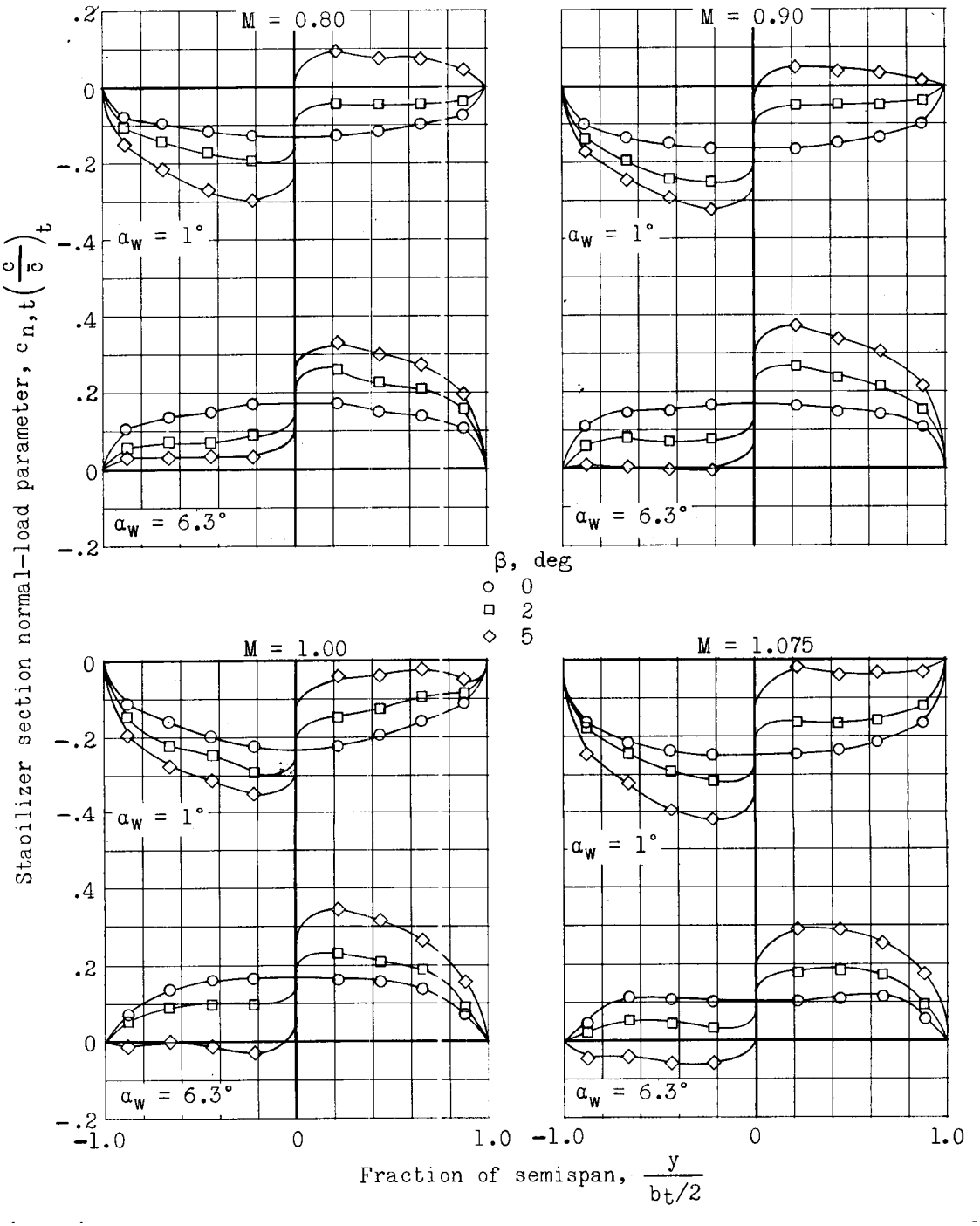

(a) Stabilizer spanwise loading.

Figure 11.- Effect of sideslip on basic-stabilizer characteristics.

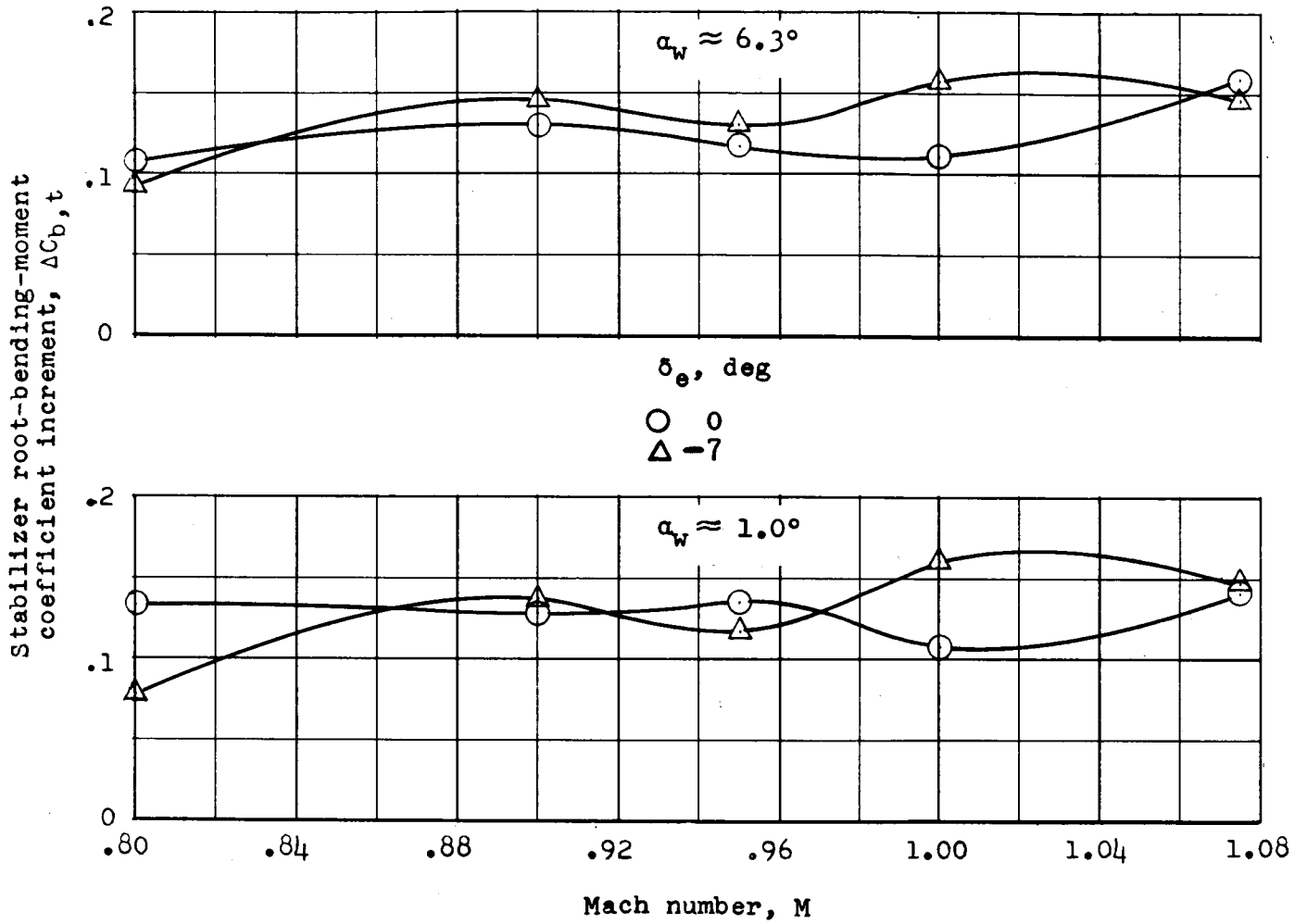

(b) Incremental stabilizer root-bending-moment coefficient due to 5° of sideslip.

Figure 11.- Continued.

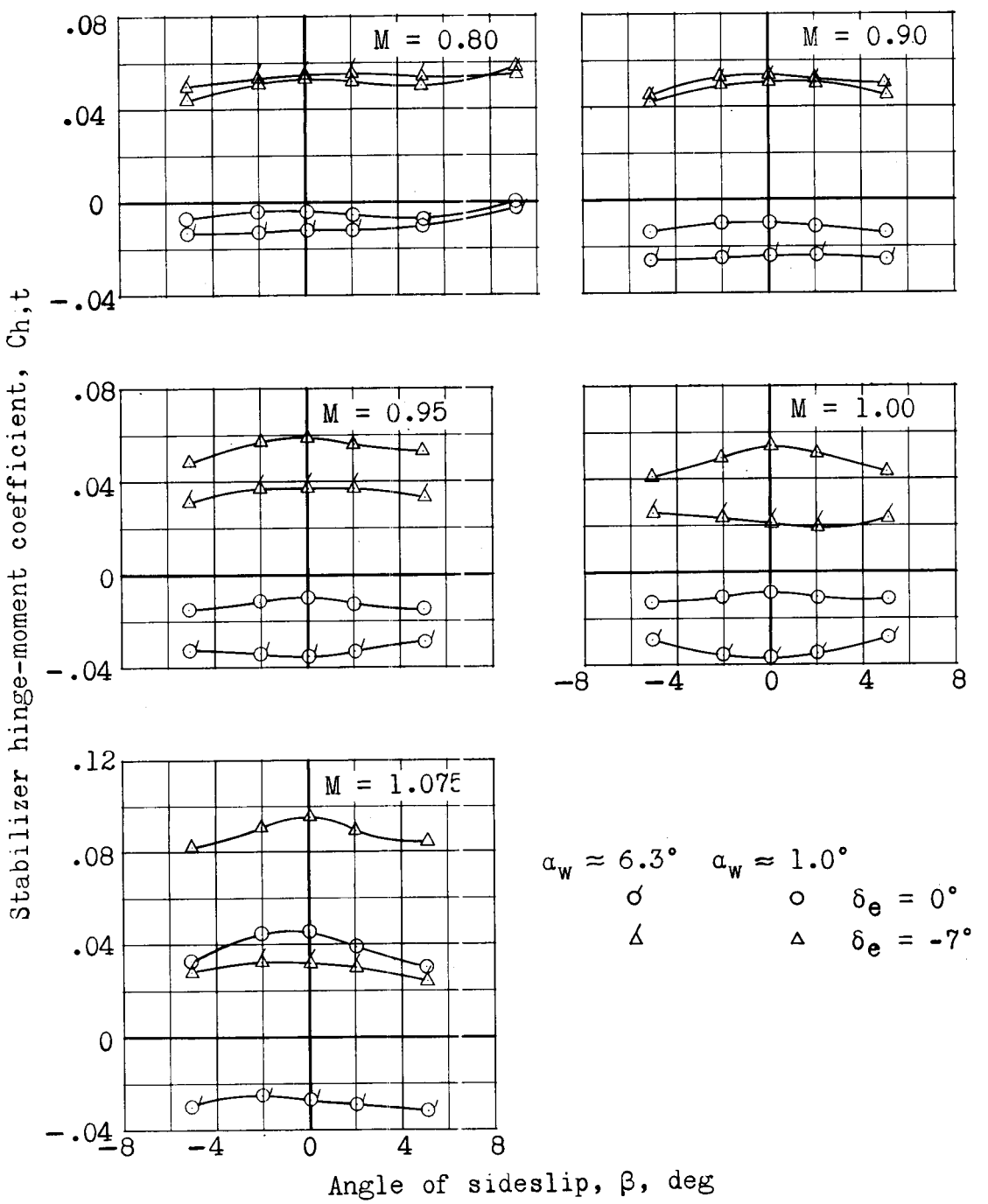

(c) Stabilizer hinge-moment characteristics.

Figure 11.- Concluded.

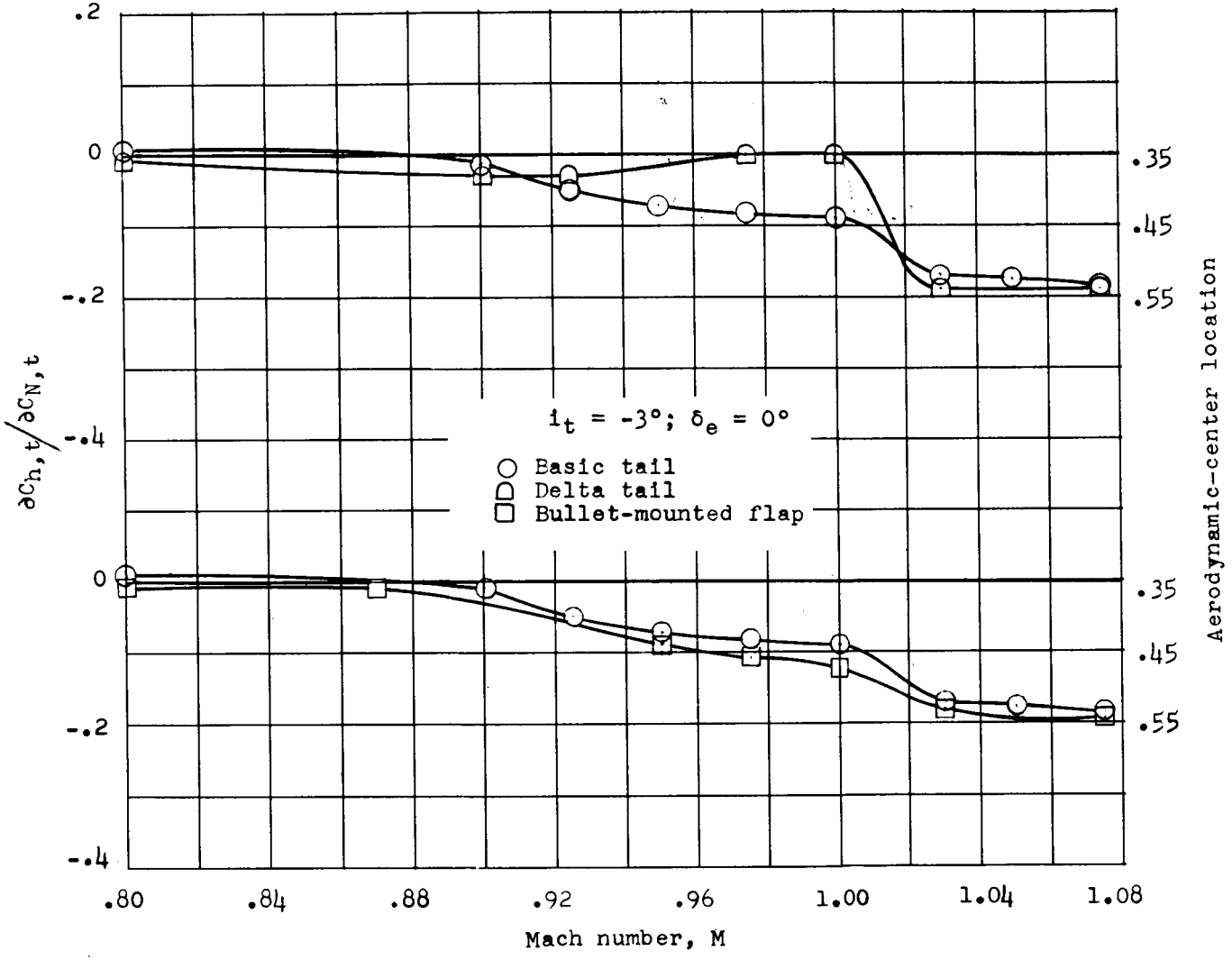

Figure 12.- Effect of modifications on $\partial C_{h,t}/\partial C_{N,t}$.

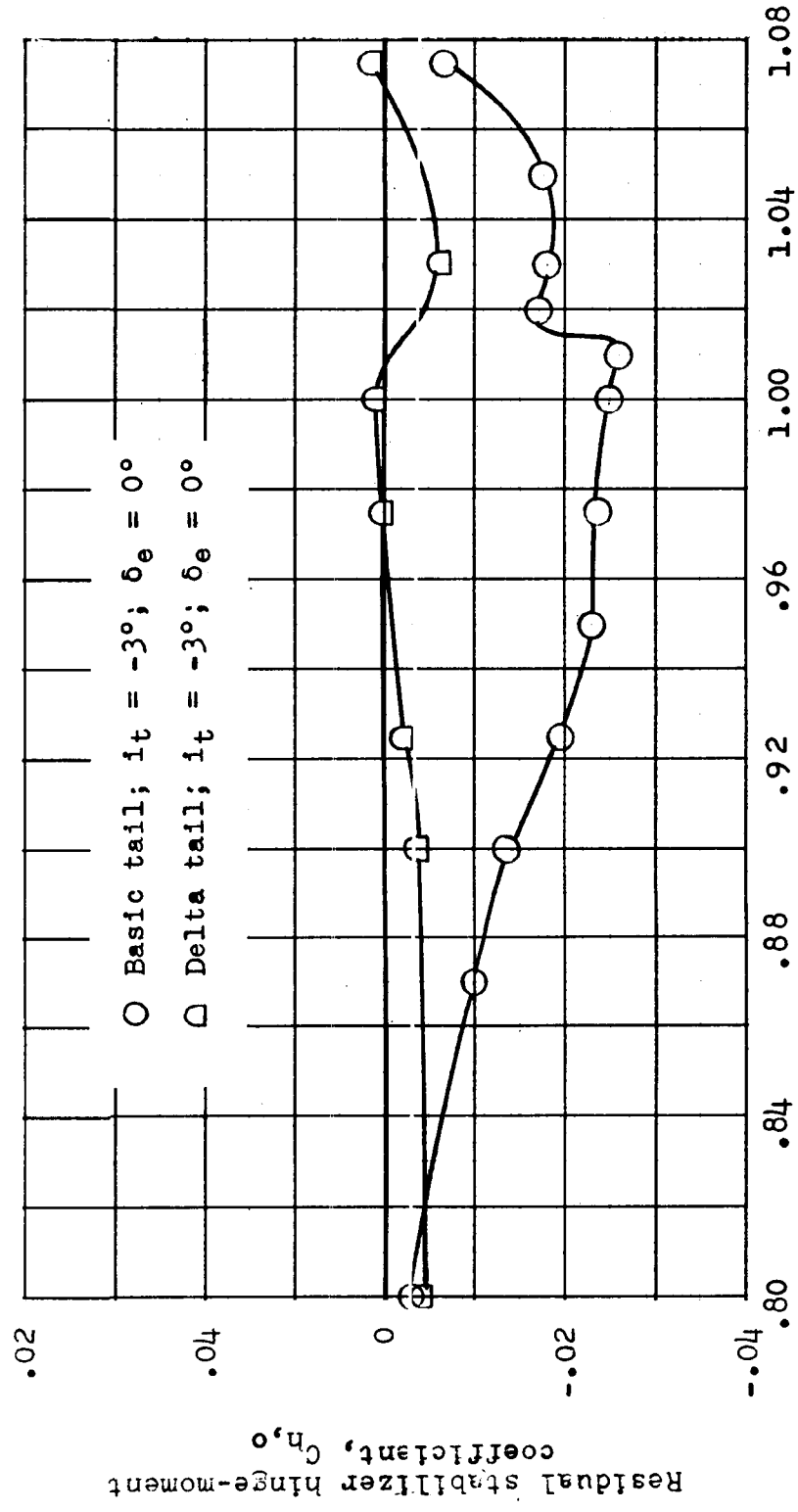

Figure 13.- Variation of residual stabilizer hinge-moment coefficient with Mach number.

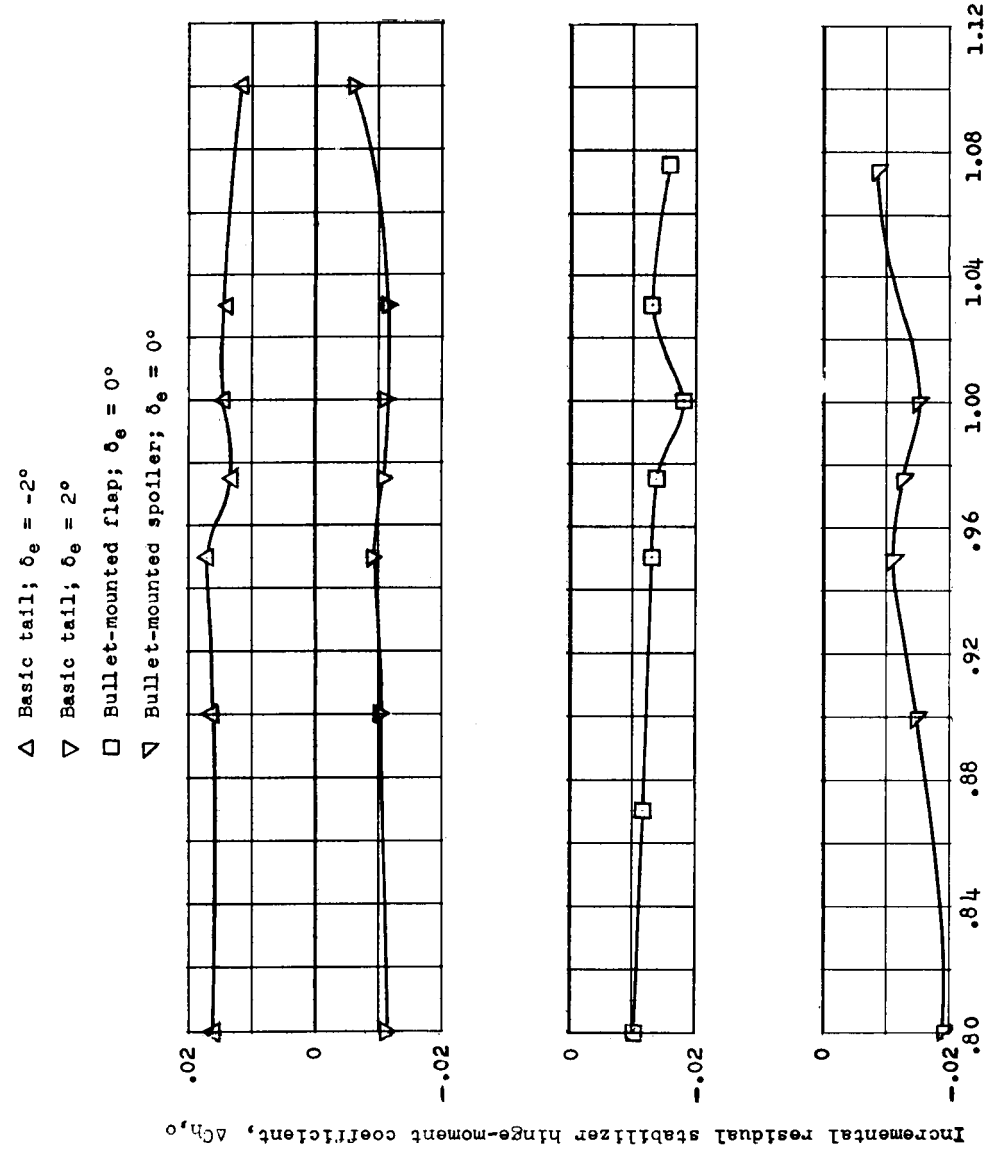

Figure 14.- Variation of incremental residual stabilizer hinge-moment coefficient with Mach number for various tail configurations.